

Micromagnetic simulation of nanoscale films with perpendicular anisotropy

U. Nowak^{a)}

Theoretische Tieftemperaturphysik, Gerhard-Mercator-Universität-Duisburg, 47048 Duisburg/Germany

A model is studied for the theoretical description of nanoscale magnetic films with high perpendicular anisotropy. In the model, the magnetic film is described in terms of single domain magnetic grains with Ising-like behavior, interacting via exchange as well as via dipolar forces. Additionally, the model contains an energy barrier and a coupling to an external magnetic field. Disorder is taken into account in order to describe realistic domain and domain wall structures. The influence of a finite temperature as well as the dynamics can be modeled by a Monte Carlo simulation. Many of the experimental findings can be investigated and at least partly understood by the model introduced above. For thin films, the magnetization reversal is driven by domain wall motion. The results for the field and temperature dependence of the domain wall velocity suggest that for thin films hysteresis can be described as a depinning transition of the domain walls rounded by thermal activation for finite temperatures.

I. INTRODUCTION

We focus on thin ferromagnetic films with high perpendicular anisotropy like CoPt and MnBi which can be used as magneto-optical storage media. In these films, two different mechanisms can be thought to dominate the reversal process: either nucleation or domain wall motion.¹ Which of these mechanisms dominates a reversal process depends on the interplay of the different interaction forces between domains with different magnetic orientations. In a recent experiment on Co₂₈Pt₇₂ alloy films,^{2,3} a crossover from magnetization reversal dominated by domain growth to a reversal dominated by a continuous nucleation of domains was found depending on the film thickness which was varied from 100 to 300 Å. Correspondingly, characteristic differences for the hysteresis loops have been found. Similar results have been achieved by simulations of a micromagnetic model using energy minimization techniques^{2,3} and Monte Carlo methods, respectively.⁴ It is the goal of this article to investigate the influence of the field and the temperature on the domain wall velocity for the case of magnetization reversal dominated by domain wall motion by a Monte Carlo simulation of a micromagnetic model.

II. MICROMAGNETIC MODEL

Co₂₈Pt₇₂ alloy films have a polycrystalline structure with grain diameters of 100–250 Å. For a theoretical description by a micromagnetic model,⁵ the film is thought to consist of cells on a square lattice with a square base of size $L \times L$ where $L=200$ Å and height h of 100 Å. Due to the high anisotropy of the Co₂₈Pt₇₂ alloy film, the grains are thought to be magnetized perpendicular to the film only with a uniform magnetization M_s which is set to the experimental value of $M_s=365$ kA/m for the saturation magnetization in these systems.⁶ The grains interact via domain wall energy and dipole interaction. The coupling of the magnetization to

an external magnetic field H is taken into account as well as an energy barrier which has to be overcome during the reversal process of a single cell.

From these considerations, it follows that the change of energy caused by reversal of a cell i with magnetization $L^2 h M_s \sigma_i$ with $\sigma_i = \pm 1$ is

$$\Delta E_i = -\frac{1}{2} L h S_w \Delta \sigma_i \sum_{(j)} \sigma_j + \frac{\mu_0}{4\pi} M_s^2 L h^2 \Delta \sigma_i \times \sum_j v(\sigma_j, r_{ij}) - \mu_0 H L^2 h M_s \Delta \sigma_i. \quad (1)$$

The first term describes the wall energy ΔE_w . The sum is over the four next neighbors and for S_w we use a value of $S_w=0.0022$ J/m² which is approximately 50% of the Bloch-wall energy S_B for this system.⁶ The reason for this reduction of the grain interaction energy compared to the Bloch-wall energy is, that the crystalline structure of the system is interrupted at the grain boundary and also that due to their irregular shape the grains are not connected via their complete surface Lh .

In the second term describing the dipole coupling ΔE_d , the sum is over all cells. r_{ij} is the distance between two cells i and j in units of the lattice constant L . For large distances, it is $v(\sigma_j, r_{ij}) = \sigma_j / r_{ij}^3$. For shorter distances, a more complicated form which is a better approximation for the shape of the cells which we consider can be determined numerically and was taken into account.

The third term describes the coupling ΔE_H to an external field H .

Additionally, an energy barrier δ_i must be considered which describes the fact that a certain energy is needed to reverse an isolated cell by domain wall motion through the grain (see also Ref. 7). We assume that during the reversal process the energy barrier has its maximum value LhS_b when the domain wall is in the center of the cell, i.e., when half of the cell is already reversed. Consequently, the energy barrier which is relevant for the reversal process is reduced to $\delta = \max(0, LhS_b - 1/2 |(\Delta E_w + \Delta E_d + \Delta E_H)|)$. The simulations are in good qualitative agreement with experiments using $S_b=0.0007$ J/m².

^{a)}Electronic mail: uli@thp.uni-duisburg.de

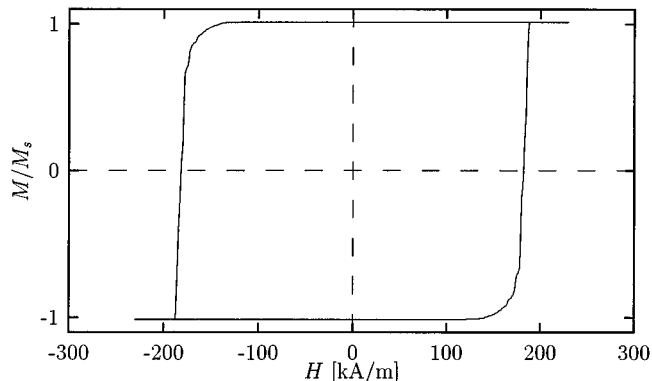


FIG. 1. Hysteresis loop for a 100 Å film; $T=300$ K.

In order to simulate the CoPt films realistically, disorder has to be considered. Obviously, the grain sizes are randomly distributed.² In the model above, this corresponds to a random distribution of L which can hardly be simulated exactly since it modulates the normalized cell distance r_{ij} of the dipole interaction. Therefore, as a simplified ansatz to simulate the influence of disorder, we randomly distribute L in the energy term that describes the coupling to the external field. Here a random fluctuation of L is most relevant, since this term is the only one scaling quadratically with L . In the simulations, we use a distribution which is Gaussian with width Δ . Note, that through this kind of disorder our model is mapped on a random-field model.

The simulation of the model above was done as in earlier publications^{4,7} via Monte Carlo methods⁸ using the Metropolis algorithm with an additional energy barrier. Since the algorithm satisfies detailed balance and Glauber dynamics, it allows the investigation of thermal properties as well as the investigation of the dynamics of the system. For temperatures $T \rightarrow 0$, the Monte Carlo algorithm passes into a simple energy minimization algorithm with single spin flip dynamics, so that also the case of zero temperature can be investigated.

The size of the lattice was typically 150×150 . The dipole interaction was taken into account without any cut-off or mean field approximation.

III. HYSTERESIS AND DYNAMICS

Figure 1 shows a simulated hysteresis loop. The loop is nearly rectangular. Here, the reversal is dominated by domain wall motion.⁴ Once a nucleus begins to grow, the domain wall motion does not stop until the magnetization has completely changed. The nucleation field for the simulation is too high compared to the corresponding experimental results.^{2,3} There are several possible reasons for this effect. First, the nucleation field, which in the case of domain wall motion dominated reversal, is the field where domain wall motion starts depends on the size and on the shape of the nucleus. In an experimental situation, a nucleus can be very large, e.g., a scratch while there is no such artificial nucleus in our simulation except of the disorder which leads only to nuclei of very small size. However, it is not the aim of our

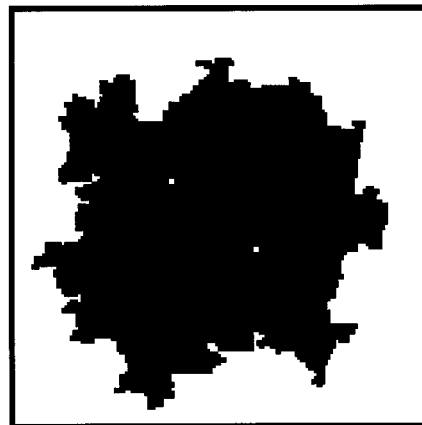


FIG. 2. Domain configuration of a 150×150 system during the reversal; $T=300$ K.

simulations to calculate the nucleation field accurately. Rather, the simulations are thought to contribute to a better understanding of the fundamental properties of the system.

Since the reversal is driven by domain wall motion, the velocity of the domain wall is a central quantity which we will investigate in the following. For the determination of the domain wall velocity within the simulation, we start with a system that has a nucleus of circular shape with a radius of 19 cells in the center of the 150×150 system. When we switch on the driving field, from the nucleus a domain starts to grow. For the better observation of the domain growth, in our flip algorithm, we do not consider cells that are not connected to the growing domain, i.e., we exclude the possibility of additional nucleation. Otherwise we have—at least for finite temperatures—the problem that spontaneously new nuclei are build by thermal activation which with increasing radius overlap with the original domain. Figure 2 shows a domain during the reversal. The black region is the reversed domain following the magnetic field. It has a circular shape with a rough domain wall. From the domain configurations, the mean radius r of the domains can be determined through the area F of the reversed domain as $r = \sqrt{F/\pi}$, assuming that the domain has a circular shape.

In order to get a deeper understanding of the influence of the temperature on the dynamics, we simulated the reversal for temperatures $T=0, 300$, and 600 K. Figure 3 shows—as an example—the $r(t)$ behavior from the simulations for $T=0$ K and different fields. For $r > 75$, the domain reaches the boundary of the system and—consequently— $r(t)$ saturates. For zero temperature, the domain wall is pinned for lower fields, i.e., after a short period of rearrangement of the domain wall the domain wall movement stops and the radius remains constant. The pinning of the domain wall is due to energy barriers which follow from the disorder, the dipole field, and the intrinsic energy barrier of the single cell. For finite temperatures, the domain wall velocity is always finite.

For $20 < r < 75$, the slope of the $r(t)$ curve is approximately constant and v can be determined by fitting to a straight line. Figure 4 shows the dependence of the domain wall velocity on the driving field for $T=0, 300$, and 600 K. For zero temperature, there is a sharp depinning transition⁹ at

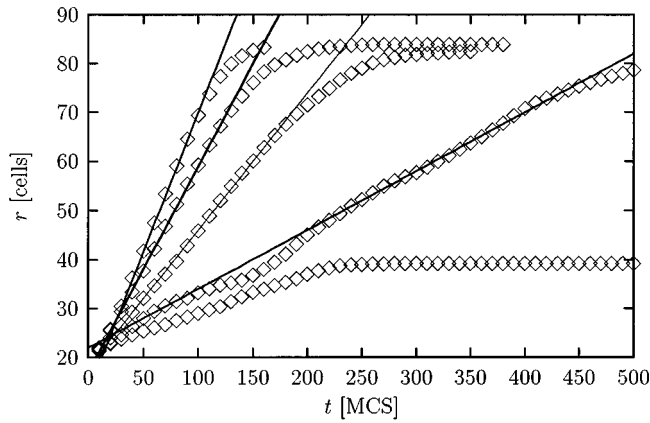


FIG. 3. Radius of the domain versus time for the same fields as in Fig. 4; $T=0$; solid lines are best fitted.

a critical field H_c from a pinned phase with $v=0$ to a phase with finite domain wall velocity. This transition can be interpreted in terms of a phase transition with $v \sim (H - H_c)^\theta$ for $H > H_c$ where in our case the critical exponent is $\theta \approx 1$, a value which is the mean field result for a moving elastic interface¹⁰ in a random field. Also, this value has been observed in simulations of a soft spin model with random fields.¹¹ For finite temperatures, the transition is smeared since for finite temperatures there is even for $H < H_c$ for each energy barrier a finite probability that the barrier can be overcome by thermal fluctuations. The corresponding waiting time can be expected to be exponentially large so that for $H < H_c$ the domain wall velocity should decrease like

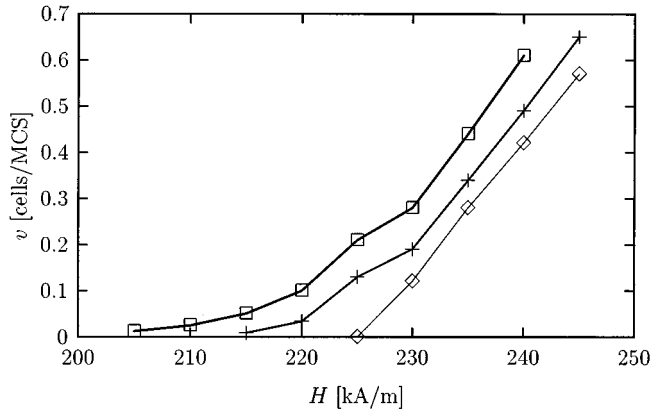


FIG. 4. Domain wall velocity vs driving field for $T=0, 300$, and 600 K; solid lines are guides to the eye.

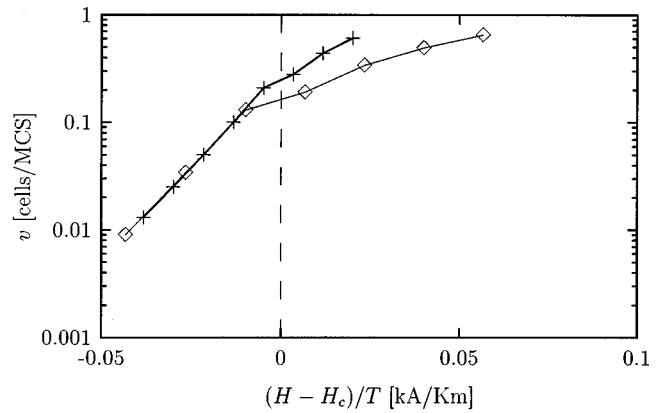


FIG. 5. Scaling plot from Fig. 4.

In $v \sim (H - H_c)/T$. To illustrate this in Fig. 5, we show the corresponding semilogarithmic scaling plot. As we expect, the data for the two different finite temperatures collapse for $H < H_c$ on a straight line. For $H > H_c$, thermal activation is obviously less relevant. Here, the dynamics is dominated by the zero temperature depinning transition.

To conclude, the results for the domain wall velocity suggest that for zero temperature the hysteresis driven by domain wall motion can be understood as a depinning transition of the domain walls. For finite temperature, the transition is rounded and for fields smaller than the depinning field the domain wall movement is dominated by thermal activation. An article on a comparison of these theoretical results with experimental measurements of the domain wall velocity in CoPt alloy films is in preparation.

ACKNOWLEDGMENT

The author thanks K. D. Usadel for helpful discussions and for critically reading the manuscript.

- ¹J. Pommier, P. Meyer, G. Pénissard, J. Ferré, P. Bruno, and D. Renard, *Phys. Rev. Lett.* **65**, 2054 (1990).
- ²T. Kleinefeld, J. Valentin, and D. Weller, *JMMM* **148**, 249 (1994).
- ³J. Valentin, T. Kleinefeld, and D. Weller, *J. Phys. D* **29**, 1111 (1996).
- ⁴U. Nowak, *IEEE Trans. Magn.* **31**, 4169 (1995).
- ⁵W. Andrä, H. Danan, and R. Mattheis, *Phys. Status Solidi A* **125**, 9 (1991).
- ⁶J. Harzer, RWTH Aachen, Ergebnisbericht (1992) (unpublished).
- ⁷U. Nowak, U. Ruediger, P. Fumagalli, and G. Güntherodt, *Phys. Rev. B* **54**, 13 017 (1996).
- ⁸K. Binder, *Monte Carlo Methods in Statistical Physics* (Springer, Berlin, 1979).
- ⁹M. Kardar and D. Ertas, in *Scale Invariance, Interfaces, and Non-Equilibrium Dynamics*, edited by A. McKane, M. Droz, J. Vannimenus, and D. Wolf (Plenum, New York, 1995), p. 89.
- ¹⁰H. Leschhorn, *J. Magn. Magn. Mater.* **104–107**, 309 (1992).
- ¹¹K. D. Usadel and M. Jost, *J. Phys. A* **26**, 1783 (1993).